Performance analyses of subcarrier BPSK modulation over M turbulence channels with pointing errors

MA Shuang (马爽)[1,2]*, **LI Ya-tian** (李亚添)[2], **WU Jia-bin** (吴佳彬)[1,2], **GENG Tian-wen** (耿天文)[2], **and WU Zhi-yong** (吴志勇)[2]

1. University of Chinese Academy of Sciences, Beijing 100049, China

2. Changchun Institute of Optics, Fine Mechanics and Physics, Chinese Academy of Sciences, Jilin 130033, China

(Received 7 March 2016)

An aggregated channel model is achieved by fitting the Weibull distribution, which includes the effects of atmospheric attenuation, M distributed atmospheric turbulence and nonzero boresight pointing errors. With this approximate channel model, the bit error rate (*BER*) and the ergodic capacity of free-space optical (FSO) communication systems utilizing subcarrier binary phase-shift keying (BPSK) modulation are analyzed, respectively. A closed-form expression of *BER* is derived by using the generalized Gauss-Lagueree quadrature rule, and the bounds of ergodic capacity are discussed. Monte Carlo simulation is provided to confirm the validity of the BER expressions and the bounds of ergodic capacity.

Document code: A **Article ID:** 1673-1905(2016)03-0221-5

DOI 10.1007/s11801-016-6054-x

Recently, free-space optical (FSO) communications have become a hot topic with plenty of advantages, such as huge bandwidth, large capacity and high security[1-5]. It is essential to build a mathematic model that accurately describes the composite probability density function (PDF). Various irradiance PDF models have been discovered to model FSO channel, such as gamma-gamma (GG)[6], log-normal (LN)[7] and K distribution. Recently, an M distribution is proposed to model the turbulence-induced fading[8]. It is valid for weak to strong turbulence conditions, and the accuracy of the distribution is confirmed by the simulation data of unbounded plane and spherical waves[9]. In Ref.[10], the bit error rate (*BER*) of binary phase shift keying (BPSK) subcarrier intensity modulated generalized FSO system has been analyzed, but the ergogic capacity is not analyzed. The channel capacity for on-off keying (OOK) modulation for M distributed channel with a tractable pointing error PDF model has been investigated in Ref.[11]. In Ref.[12], the average *BER* performance has been derived for the composite M distributed fading channel in the OOK modulation scheme. Moreover, the pointing errors in the above literature only consider the jitter of the building. In Ref.[13], the nonzero boresight pointing error model has been proposed for urban FSO links. It is used with the M distributed PDF in order to analyze the outage probability of FSO links with relays in Ref.[14].

In this paper, the *BER* performance and the ergodic capacity of subcarrier BPSK modulation are analyzed in the FSO system over an M distribution channel with the nonzero boresight pointing error model. The Weibull curve fitting is used for the PDF of the channel gain in order to derive the closed-form expression of *BER*. Besides, the upper and lower bounds of the ergodic capacity are obtained by an approximate way, respectively.

A point-to-point (P2P) link is considered for the FSO system. At the transmitter, the data source $d(t)$ is premodulated into the radio frequency (RF) signal $m(t)$. Without loss of generality, it's assumed that the power of $m(t)$ is normalized to 1. If the intensity modulation (IM) is utilized, the transmit power $P_t(t)$ can be written as $P_t(t)=P[1+\xi m(t)]$,where P defines the direct current (DC) power, and ξ stands for the modulation index. It's satisfied that $-1<\xi m(t)<1$ so as to avoid over modulation, if it's properly biased. It also should be noticed that the average power is equal to P, if $m(t)$ is modulated in BPSK scheme.

In the receiver end, the received optical power is converted into the electrical signal through direct detection (DD) at the photodetector. Assuming $h(t)$ to be the channel gain of the P2P link, the received electrical signal $y(t)$ of photodetector can be written as[3]

$$y(t)=Rh(t)\cdot P_t(t)+n(t), \tag{1}$$

where R stands for the photodetector responsivity, $n(t)$ is the equivalent noise including thermal noise and shot noise at the receiver, which can be modeled as additive white Gaussian noise (AWGN).

For the convenience, it's assumed that h is short for the value of $h(t)$ at the sample time t_0, which means $h=h(t_0)$. In the similar way, it's defined that $P_t=P_t(t_0)$, $n=n(t_0)$ and $y=y(t_0)$. In this simplification, the propagation delay is

* E-mail: jy01892231@126.com

ignored. The output signal-to-noise ratio (*SNR*) γ can be given as

$$\gamma=\frac{(PR\xi)^2}{\sigma_{\mathrm{n}}^2}\cdot h^2=\overline{\gamma}\cdot h^2, \tag{2}$$

where σ_{n} is the noise standard deviation, and $\overline{\gamma}$ is defined as the *SNR* without fading assuming normalized channel gain.

In this paper, a compound channel model is considered, which is made up of atmospheric attenuation h_1, pointing error h_{p} and atmospheric turbulence h_{a}, i.e., $h=h_1\cdot h_{\mathrm{a}}\cdot h_{\mathrm{p}}$. In the FSO system, the atmospheric attenuation h_1 can be calculated by the exponential Beers-Lambert law, which is

$$h_1(z)=\exp(-\sigma z), \tag{3}$$

where z denotes the propagation distance, and σ is the atmospheric attenuation coefficient.

The atmospheric turbulence h_{a} follows an M distribution based on the distinction between the classic scattering fields. The PDF of h_{a} can be written as[15]

$$f_{h_{\mathrm{a}}}(h_{\mathrm{a}})=B\sum_{k=1}^{\beta}b_k(h_{\mathrm{a}})^{\frac{\alpha+k}{2}-1}K_{\alpha-k}\left(2\sqrt{\frac{\alpha\beta h_{\mathrm{a}}}{\zeta_{\mathrm{g}}\beta+\Omega'}}\right), \tag{4}$$

and

$$\begin{cases} B\approx\dfrac{2\alpha^{\frac{\alpha}{2}}}{\zeta_{\mathrm{g}}^{1+\frac{\alpha}{2}}\Gamma(\alpha)}\left(\dfrac{\zeta_{\mathrm{g}}\beta}{\zeta_{\mathrm{g}}\beta+\Omega'}\right)^{\beta+\frac{\alpha}{2}} \\ b_k\approx\dbinom{\beta-1}{k-1}\dfrac{(\zeta_{\mathrm{g}}\beta+\Omega')^{1-\frac{k}{2}}}{\Gamma(k)}\left(\dfrac{\Omega'}{\zeta_{\mathrm{g}}}\right)^{k-1}\left(\dfrac{\alpha}{\beta}\right)^{\frac{k}{2}} \end{cases}, \tag{5}$$

where α represents the effective number of large-scale cells of the scattering process which is a positive parameter, and β denotes the amount of fading parameter which is a nature number. $\zeta_{\mathrm{g}}=\mu\zeta$ stands for the average optical power of classic scattering component received by off-axis eddies, where ζ is the average power of the total scatting components, and $0<\mu<1$ is a scale factor. Ω' denotes the average optical power of coherent contributions, which is the line of sight (LOS) component and the coupled-to-LOS scattering term. $\Gamma(\cdot)$ is the Gamma function, and $K_i(\cdot)$ is the modified Bessel function of the second kind with the order i.

Both the boresight and the jitter are considered, the PDF of the nonzero boresight pointing error h_{p} is given as

$$f_{h_{\mathrm{p}}}(h_{\mathrm{p}})=\frac{\rho^2\exp\left(-\frac{s^2}{2\sigma_{\mathrm{s}}^2}\right)}{A_0^{\rho^2}}(h_{\mathrm{p}})^{\rho^2-1}I_0\left(\frac{s}{\sigma_{\mathrm{s}}^2}\sqrt{-\frac{w_{\mathrm{zeq}}^2\log\left(\frac{h_{\mathrm{p}}}{A_0}\right)}{2}}\right), \tag{6}$$

where A_0 is the fraction of the collected power when the detector center satisfies r=0. A_0 can be derived as $A_0=erf^2(v)$, where $v=\sqrt{\pi}a/(\sqrt{2}w_z)$ represents the ratio between aperture radius a and beam width w_z, and $erf(\cdot)$ denotes the error function. $w_{z\mathrm{eq}}$ strands for the equivalent beam width, which can be calculated by $w_{\mathrm{zeq}}^2=w_z^2\sqrt{\pi}erf(v)\big/\left[2v\exp(-v^2)\right]$, and $I_0(\cdot)$ denotes the zero-order modified Bessel function of the first kind. $\rho=w_{\mathrm{zeq}}\big/\left(\sqrt{2}w_z\right)$, s is the zero boresight error, and σ_{s} is the jitter standard deviation at the receiver.

Considering the independence of h_1, h_{a} and h_{p}, the PDF of h could derived as[16]

$$\begin{aligned} f_h(h)=&\frac{2\pi B\rho^2\exp(\frac{s^2}{2\sigma_{\mathrm{s}}^2})}{w_{\mathrm{zeq}}^2}\sum_{k=1}^{\beta}\frac{b_k h^{\frac{\alpha+k}{2}-1}}{(A_0h_1)^{\frac{\alpha+k}{2}}\sin[\pi(\alpha-k)]}\times \\ &\sum_{p=0}^{\infty}\left\{\frac{\left[\frac{\alpha\beta h}{(\zeta_{\mathrm{g}}\beta+\Omega')A_0h_1}\right]^{p-\frac{\alpha-k}{2}}}{\Gamma\left[p-(\alpha-k)+1\right]p!}\times\right. \\ &\int_0^x x\left[\exp\left(\frac{2x^2}{w_{\mathrm{zeq}}^2}(p+k-\rho^2)\right)-\right. \\ &\left.\left.\exp\left(\frac{2x^2}{w_{\mathrm{zeq}}^2}(p+\alpha-\rho^2)\right)\right]I_0\left(\frac{s}{\sigma_{\mathrm{s}}^2}x\right)\mathrm{d}x\right\}. \end{aligned} \tag{7}$$

However, the PDF of h is too complex to calculate the theoretical values of *BER* and the ergodic capacity. Instead, a simplification method is illustrated.

The Weibull PDF was introduced as a generalization of the exponential PDF, which originally appeared in the field of reliability engineering[15]. Recently, the Weibull distribution has been used to propose a double-Weibull process, in order to describe the PDF of the irradiance fluctuations in moderate and strong regimes of turbulence[16], besides in wireless communication where some channels are modeled with Weibull fading[17]. It's proposed that the Weibull PDF becomes a useful distribution to model the received power fluctuations in an optical link through the atmospheric turbulence under aperture averaging conditions[18].

The curve fitting is utilized to approach the channel gain h. Taking the monotony of PDFs of h_{a} and h_{p} into consideration, Weibull distribution is proposed to fit the PDF of h. And the PDF $\tilde{f}_h(h)$ of Weibull distribution is given as

$$\tilde{f}_h(h)=\frac{k}{\lambda}\left(\frac{h}{\lambda}\right)^{k-1}\cdot\exp\left[-\left(\frac{h}{\lambda}\right)^k\right],\ x\geq 0\ , \tag{8}$$

where λ stands for the shape parameter, and k denotes the scale parameter. Both λ and k need to be positive. It needs to be noticed that each group of (λ, k) is corresponding to one kind of atmospheric channel with pointing errors. That is, λ and k are both influenced by σ, σ_s, w_z, α, β, ζ_g, Ω', s, a and z.

Fig.1 shows the curve fitting distributions of Weibull PDF $\tilde{f}_h(h)$ and the density histograms of the channel gain h in the simulation, while the simulation parameters are given in Tab.1.

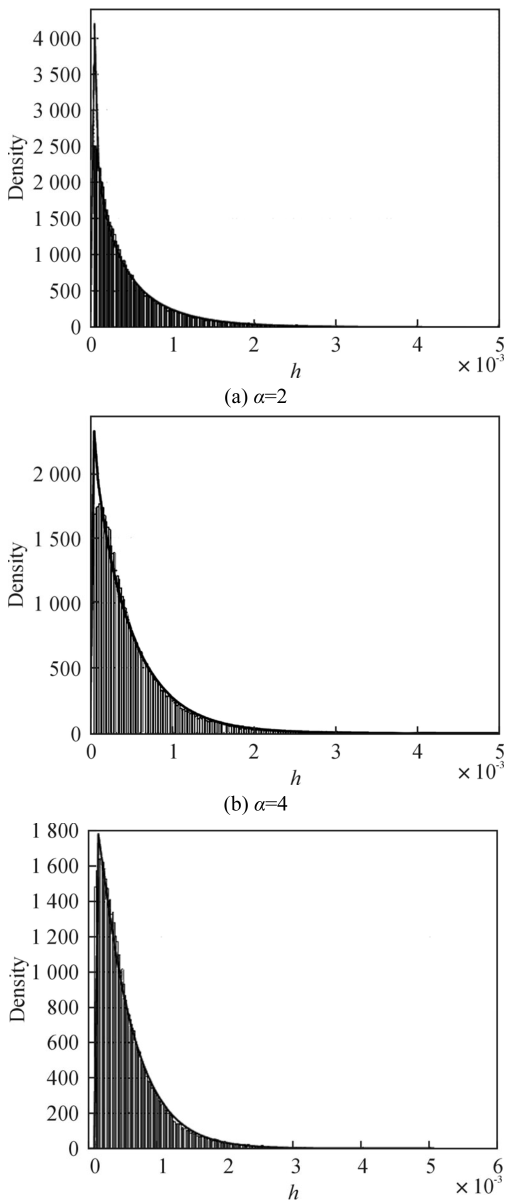

(a) α=2

(b) α=4

(c) α=6

Fig.1 Density histograms of the channel gain *h* in simulation with *α*=2, 4 and 6 and corresponding curve fitting distributions of Weibull PDF

It can be derived from Fig.1 that the Weibull distribution almost fits the channel gain perfectly as a whole. Moreover, when h is smaller than about 10^{-4}, the probability density values in fitting curves are a little larger than those in corresponding histograms.

The statistics parameters of the fitting and simulation are given in Tab.2. It illustrates that the fitting results (both mean and variance of h) are approximate to those simulation results.

Tab.1 Simulation parameters

Parameter	Value
Optoelectronic conversion factor R (A/W)	0.5
Modulation index ξ	0.9
Noise standard deviation σ_n (A/Hz)	10^{-7}
Atmospheric attenuation coefficient σ (dB/km)	8
Jitter standard deviation σ_s (m)	0.2
Beam width w_z (m)	2.5
Effective number of large-scale cells α	2, 4, 6
Amount of fading parameter β	2
Average optical power of classic scattering component received by off-axis eddies ζ_g	0.2
Average optical power of coherent contributions Ω'	0.8
Zero boresight error s (m)	0.3
Aperture radius a (m)	0.1
Propagation distance z (km)	1

Tab.2 Statistics parameters of fitting and simulation

Parameter	α=2	α=4	α=6
Scale parameter λ ($\times10^{-4}$)	4.380	4.748	4.862
Shape parameter k ($\times10^{-1}$)	8.660	9.785	1.034
Mean of h by simulation ($\times10^{-4}$)	4.797	4.700	4.797
Mean of h by fitting ($\times10^{-4}$)	4.710	4.793	4.796
Variance of h by simulation ($\times10^{-7}$)	3.116	2.376	2.214
Variance of h by fitting ($\times10^{-7}$)	2.978	2.399	2.312

In order to achieve the expectation value $P_{\rm e\_th}$ of BER, the conditional BER is considered for the BPSK modulation, which can be expressed as

$$P_{\rm e}\left(h\right)=Q\left(\sqrt{2\overline{\gamma}h^2}\right), \tag{9}$$

where $Q(\cdot)$ denotes the Gaussian Q function. And the expectation value $P_{\rm e\_th}$ can be calculated by

$$P_{\rm e\_th}=\int_0^\infty Q\left(\sqrt{2\overline{\gamma}h^2}\right)\tilde{f}_h\left(h\right){\rm d}h\,. \tag{10}$$

For convenience, assume that $z=R^2P_{\rm t}^2h^2/\left(2\sigma_n^2\right)$. Then Eq.(10) can be expressed as

$$P_{\rm e\_th}=\frac{\sigma_{\rm n}}{\sqrt{2\pi}RP_{\rm t}}\int_0^\infty z^{-1/2}{\rm e}^{-z}\left\{1-\exp\left[-\frac{\sqrt{2}\sigma_{\rm n}}{RP\lambda}\sqrt{z}\right]^k\right\}{\rm d}z\,. \tag{11}$$

Note that Eq.(11) has the form of $\int_0^\infty x^a{\rm e}^{-x}f\left(x\right){\rm d}x$. In order to derive the closed-form expression of $P_{\rm e\_th}$, the generalized Gauss-Lagueree quadrature rule is utilized. And Eq.(11) can be changed as

$$P_{\mathrm{e\_th}}=\frac{\sigma_n}{\sqrt{2\pi}RP_{\mathrm{t}}}\sum_{m=1}^{n}W_m\left\{1-\exp\left[-\frac{\sqrt{2}\sigma_n}{RP\lambda}\sqrt{z_m}\right]^k\right\}, \quad (12)$$

where z_m is the mth root of the generalized Laguerre polynomial $L_n^{-1/2}(z)$, and the weight W_m is given by

$$W_m=\frac{\Gamma(n+1/2)z_m}{n!(n+1)^2\left[L_{n+1}^{-1/2}(z_m)\right]^2}, \quad (13)$$

where $\Gamma(\cdot)$ denotes Gamma function with $\Gamma(x)=\int_0^{\infty}t^{x-1}\mathrm{e}^{-t}\mathrm{d}t$.

The ergodic capacity is proposed to measure the effectiveness of a communication system if the channel gain h changes quickly enough, i.e., all the data in one set can experience all the possible value of h, which seems not suitable for the FSO system. However, interleaving makes it possible for a set of data to experience all the possible values of h with enough interleaving depth. And the expectation of the ergodic capacity is given as

$$E(C)=\int_0^{\infty}\log_2\left[1+\frac{(PR\xi)^2}{\sigma_{\mathrm{n}}^2}\cdot h^2\right]\tilde{f}_h(h)\mathrm{d}h. \quad (14)$$

It's still too complex to derive the closed-form theoretical result of Eq.(14). As a result, the bounds of the ergodic capacity are discussed below. Due to the concavity of the ergodic capacity, Jensen's inequality is utilized, which is

$$E(C)=E\left\{\log_2\left[1+\frac{(PR\xi)^2}{\sigma_{\mathrm{n}}^2}h^2\right]\right\}\le$$

$$\log_2\left[1+\frac{(PR\xi)^2}{\sigma_{\mathrm{n}}^2}E(h^2)\right] , \quad (15)$$

and it can be simplified as

$$E(C)\le\log_2\left\{1+\frac{(PR\xi)^2}{\sigma_{\mathrm{n}}^2}\cdot\left(\mathrm{var}(h)+\left[E(h)\right]^2\right)\right\}. \quad (16)$$

After obtaining the upper bound, the lower bound of Eq.(14) can be derived as

$$E(C)=E\left\{\log_2\left[1+\frac{(PR\xi)^2}{\sigma_{\mathrm{n}}^2}h^2\right]\right\}\ge$$

$$E\left\{\log_2\left[\frac{(PR\xi)^2}{\sigma_{\mathrm{n}}^2}h^2\right]\right\}^+ , \quad (17)$$

where $\{x\}^+$ means the maximum of x and 0, in order to avoid $E(C)$<0 when the transmit power P_{t} is not larger enough to ensure $\frac{(PR\xi)^2}{\sigma_{\mathrm{n}}^2}\cdot h^2>1$.

Eq.(17) can also be written as the form of

$$E(C)\ge\left\{E\left[\log_2\left(\frac{(PR\xi)^2}{\sigma_{\mathrm{n}}^2}h^2\right)\right]\right\}^+=$$

$$\left\{\frac{2\ln\lambda}{\ln 2}+\log_2\left[\frac{(PR\xi)^2}{\sigma_{\mathrm{n}}^2}\right]\right\}^+. \quad (18)$$

So Eqs.(16) and (18) illustrate the bounds of ergodic capacity.

The simulation results and the theoretical results are analyzed as follows. The simulation parameters are given in Tab.2. The *BER* performances are described in Fig.2 with the increase of average transmit power P_{t}. As shown in Fig.2, the theoretical results are in accord with the simulation results. The *BER* has a better performance when the transmit power P_{t} increases.

It can be obtained from Fig.2 that the *BER* performance gets better with the increase of w_z/a. However, the difference between simulation and theoretical results becomes larger, when the transmit power P_{t} is greater than a threshold, which is 0 dBm in Fig.2. When the transmitting power P_{t} is smaller than the threshold, $\bar{\gamma}$ is mainly influenced by P_{t}. However, with the further increase of P_{t}, the channel gain h mainly influences the *BER* performance. As described in Fig.1, the probability of h in the PDF fitting curve is larger than that in simulation when h is not larger enough, which is consistent with the results in Tab.1. That's why the theoretical curve departures from the simulation with larger P_{t}.

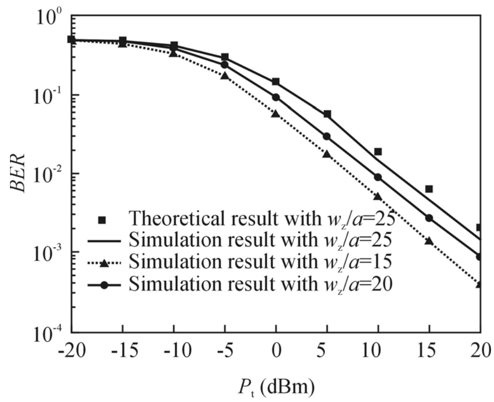

Fig.2 Simulation and theoretical *BER* performances versus the average transmit power P_{t} with different w_z/a

Fig.3 shows the *BER* performances for the subcarrier BPSK FSO systems with different zero boresight errors s when the other simulation parameters are the same as those in Tab.2. It can be concluded from Fig.3 that, with the increase of s, the energy collected at receiver aperture decreases, which makes the *BER* performance worse.

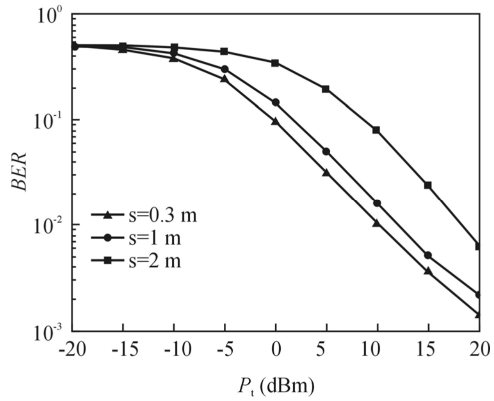

Fig.3 *BER* performance versus the average transmit power P_t with different zero boresight errors *s*

The capacity performance is shown in Fig.4. The theoretical result accurately coincides with the simulation result. Moreover, both the simulation and theoretical results almost lie between the upper and lower bounds of $E(C)$. As discussed above, the mean value satisfies that $E(\tilde{h}) < E(h)$, and the PDF of $\tilde{h}$ is greater than that of h when h is small. While, the PDF of $\tilde{h}$ is smaller than that of h when h becomes larger. As a result, the simulation result is greater than the upper bound.

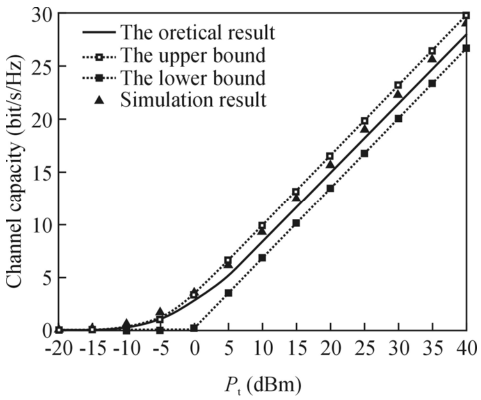

Fig.4 Capacity performance and its bounds versus the average transmit power P_t

It's also noted in Fig.4 that the lower bound is zero when P_t is smaller than −5 dBm. Due to the fact that the lower bound in Eq.(18) is in the form $\{x\}^+$, $(PR\xi)^2 \cdot h^2 / \sigma_n^2 < 1$ can result in the lower bound of 0. And it can be estimated that the threshold of the transmission power is $P_{th}=\sigma_n/(hR\xi)$.

In conclusion, the *BER* and the ergodic capacity performances of subcarrier BPSK modulation over atmospheric turbulence channel with pointing errors are investigated. An aggregated channel model, including the effects of atmospheric attenuation, M distributed atmospheric turbulence and nonzero boresight pointing errors, is considered, and an approximate model is achieved by fitting the Weibull distribution. A closed-form expression of *BER* is derived by utilizing the generalized Gauss-Lagueree quadrature rule, and the bounds of ergodic capacity are discussed. Numerical results show that the derived theoretical expressions of the *BER* and the bounds of ergodic capacity can be utilized to approximate the simulation results almost perfectly.

References

[1] J. Y. Wang, J. B. Wang, M. Chen, N. Huang, L. Q. Jia and R. Guan, Optical Engineering **53**, 016107 (2014).

[2] J. Zhang, M. A. Itzler, H. Zbinden and J. W. Pan, Light: Science & Applications **4**, e286 (2015).

[3] X. Yi and M. Yao, Optics Express **23**, 2904 (2015).

[4] LI Ming, HUANG Yong, GAO Yang and YANG Shaowen, Journal of Optoelectronics·Laser **25**, 1310 (2014). (in Chinese)

[5] ZHAO Qingsong, HAO Shiqi, GENG Hong-jian, LIU Jia-lin, WANG Yong and SUN Han, Journal of Optoelectronics·Laser **26**, 1081 (2015). (in Chinese)

[6] T. Cao, P. Wang, L. Guo, B. Yang, J. Li and Y. Yang, Chinese Optics Letters **13**, 080101 (2015).

[7] M. Abaza, R. Mesleh, A. Mansour and E. H. Aggoune, Chinese Optics Letters **13**, 051001 (2015).

[8] A. Jurado-Navas, J. Garrido-Balsells, J. Paris and A. Puerta-Notario, A Unifying Statistical Model for Atmospheric Optical Scintillation, Numerical Simulations of Physical and Engineering Processes, 181 (2011).

[9] H. E. Nistazakis, A. N. Stassinakis, H. G. Sandalidis and G. Tombras, IEEE Photonics Journal **7**, 7900411 (2015).

[10] V. K. Jagadeesh, V. Palliyembil, P. Muthuchidambaranathan and F. M. Bui, Channel Capacity and Outage Probability Analysis of Sub Carrier Intensity Modulated BPSK System over M-distribution Free Space Optical Channel, 2nd International Conference on Electronics and Communication Systems, 1051 (2015).

[11] José María Garrido-Balsells, Antonio Jurado-Navas, José Francisco Paris, Miguel Castillo-Vázquez and Antonio Puerta-Notario, Optics Letters **38**, 3984 (2013).

[12] A. Jurado-Navas, J. Garrido-Balsells, J. Paris, M. Castillo-Vázquez and A. Puerta-Notario, Optics Express **20**, 12550 (2012).

[13] F. Yang, J. Cheng and T. A. Tsiftsis, IEEE Transaction Communications **62**, 713 (2014).

[14] J. Wang, J. Wang, M. Chen, Y. Tang and Y. Zhang, IEEE Photonics Journal **6**, 790 (2013).

[15] W. Weibull, Journal of Applied Mechanics **18**, 293 (1951).

[16] N. D. Chatzidiamantis, H. G. Sandalidis, G. K. Karagiannidis, S. A. Kotsopoulos and M. Matthaiou, New Results on Turbulence Modeling for Free-Space Optical Systems, IEEE 17th International Conference on Telecommunications, 487 (2010).

[17] M. Lupupa and M. E. Dlodlo, Performance of MIMO System in Weibull Fading Channel - Channel Capacity Analysis, IEEE EUROCON, 1735 (2009).

[18] R. Barrios and F. Dios, Optics Express **20**, 13055 (2012).